OPEN

Citation: Human Genome Variation (2015) 2, 15043; doi:10.1038/hgv.2015.43
Official journal of the Japan Society of Human Genetics 2054-345X/15

www.nature.com/hgv

DATA REPORT

A novel *COL11A1* mutation affecting splicing in a patient with Stickler syndrome

Tomohiro Kohmoto[1,2,5], Takuya Naruto[1,5], Haruka Kobayashi[1,2,5], Miki Watanabe[1,2], Nana Okamoto[3], Kiyoshi Masuda[1], Issei Imoto[1] and Nobuhiko Okamoto[4]

Stickler syndrome is a clinically and genetically heterogeneous collagenopathy characterized by ocular, auditory, skeletal and orofacial abnormalities, commonly occurring as an autosomal dominant trait. We conducted target resequencing to analyze candidate genes associated with known clinical phenotypes from a 4-year-old girl with Stickler syndrome. We detected a novel heterozygous intronic mutation (NM_001854.3:c.3168+5G > A) in *COL11A1* that may impair splicing, which was suggested by *in silico* prediction and a minigene assay.

Human Genome Variation (2015) **2,** 15043; doi:10.1038/hgv.2015.43; published online 12 November 2015

Stickler syndrome, first reported by Stickler *et al.*,[1] comprises a clinically and genetically heterogeneous group of heritable connective tissue disorders characterized by ocular, auditory, skeletal and orofacial abnormalities.[2] Its incidence among neonates is ~1 in 7,500–9,000. The typical mode of inheritance is autosomal dominant; heterozygous mutations in *COL2A1* (OMIM# 120140), *COL11A1* (OMIM# 120280) and *COL11A2* (OMIM# 120290) cause Stickler syndrome types 1 (OMIM# 108300), 2 (OMIM# 604841) and 3 (OMIM# 184840), respectively.[3–5] The differential diagnosis is made according to the patient's clinical characteristics, but may sometimes be difficult because of the phenotypic variability. The diagnosis can be confirmed using molecular genetic analysis.

Standard Sanger sequencing, which is routinely used to identify pathogenic mutations, is laborious, expensive and time consuming, particularly when applied to the analysis of large genes, including those coding collagens, with numerous exons and for multiple genes that are possibly responsible for genetic diseases. Targeted next-generation sequencing (NGS) of candidate and/or known pathogenic genes can be used to overcome problems associated with Sanger sequencing to diagnose patients with disorders, including Stickler syndrome.[6] We report the use of targeted NGS to study a Japanese patient with Stickler syndrome and the identification of a novel heterozygous *COL11A1* intronic mutation outside of the highly conserved AG–GT dinucleotides, NM_001854.3:c.3168+5G > A. The mutation was present in a targeted exome panel comprising the coding regions of 4,813 clinical phenotype-associated genes, including Stickler syndrome-related genes. The functionally significant effects of this mutation on the splice donor site were revealed through *in silico* analysis and functional experiments using a minigene assay, and suggested that this mutation was the cause of Stickler syndrome in this patient.

The subject was a 4-year-old girl. She was born to healthy nonconsanguineous Japanese parents after 38 weeks of gestation. At birth, she weighed 2,260 g (−1.9 s.d.), she was 49 cm (+0.3 s.d.) in height, and her occipitofrontal circumference (OFC) was 32 cm (−0.6 s.d.). She was born with a cleft palate and short extremities. X-ray imaging at 2 years of age revealed lumbar spine lordosis, L-1 hypoplasia and metaphyseal widening of the long bones (Figure 1). Plastic surgery for cleft palate was successfully performed. Eardrum tubing was placed to alleviate otitis media with effusion and hearing loss. Her motor and mental development was normal. She demonstrated dysmorphic features, including a flat nasal bridge, short nose with anteverted nostrils, shallow orbits and prominent eyes. Ophthalmological assessment revealed bilateral high myopia (−12 diopters) and vitreoretinal degeneration. Her clinical characteristics of orofacial, ocular, auditory and skeletal abnormalities were compatible with those of Stickler syndrome. At her last examination, her height, weight and OFC were 97.3 cm (−2.0 s.d.), 16.4 kg (−0.4 s.d.), and 50.5 cm (+0.5 s.d.), respectively. No clinical characteristics of orofacial, ocular, auditory and skeletal abnormalities were detected in the parents.

The ethics committees of Tokushima University approved this study. After obtaining informed consent from her parents, a molecular diagnosis was performed using genomic DNA extracted from the patient's whole blood. Because several genes with numerous exons cause Stickler syndrome or related diseases, we first used a MiSeq benchtop sequencer (Illumina, San Diego, CA, USA) to perform NGS with a TruSight One Sequencing Panel (Illumina). The alignments of sequencing reads to the human reference genome (hg19), duplicate read removal, local realignment around indels, base quality score recalibration, variant calling and annotation were performed as described elsewhere.[7] To identify single-nucleotide variations, we excluded sequence variants with minor allele frequencies > 0.05 included in the 1,000 Genomes Project database (http://www.1000 genomes.org/), NHLBI GO Exome Sequencing Project (ESP6500, http://evs.gs.washington.edu/EVS/) and Human Genetic Variation Database

[1]Department of Human Genetics, Institute of Biomedical Sciences, Tokushima University Graduate School, Tokushima, Japan; [2]Student Lab, Faculty of Medicine, Tokushima University, Tokushima, Japan; [3]Department of Oral and Maxillofacial Surgery, Kobe University Graduate School of Medicine, Kobe, Japan and [4]Department of Medical Genetics, Osaka Medical Center and Research Institute for Maternal and Child Health, Osaka, Japan.
Correspondence: I Imoto (issehgen@tokushima-u.ac.jp)
[5]These authors contributed equally to this work.
Received 17 August 2015; revised 12 September 2015; accepted 14 September 2015

(HGVD, http://www.genome.med.kyoto-u.ac.jp/SnpDB/). Detection of copy-number alteration using NGS data with a resolution of a single exon to several exons depending on the exon size was performed as described elsewhere.[7]

These analyses identified one heterozygous mutation, NM_001854.3:c.3168+5G > A (NC_000001.10:g.103427417C > T), within an intronic sequence (intron 41) of *COL11A1* (NM_001854.3; Figure 2a). No other potentially pathogenic mutations, including variants and gross deletions, were detected in genes potentially responsible for Stickler syndrome or related diseases. This mutation is evolutionarily conserved in mammals, chickens and zebrafish (Supplementary Figure S1) and is not present in dbSNP138, 1000 Genomes Project, ESP6500 or HGVD. Although 25 point mutations, including 4 at the +3 position and 4 at the +5 position and 1 small insertion of the 73 mutations were listed as mutations located within the flanking intronic sequences that possibly affect normal splicing in Human Gene Mutation Database Professional 2015.2 (HGMD, http://www.hgmd.org/), this mutation is not present in HGMD and ClinVar (http://www.ncbi.nlm.nih.gov/clinvar/), suggesting that it is a novel mutation responsible for Stickler syndrome. Because parental DNA was not available, the mutation was not confirmed as occurring *de novo*.

To evaluate the pathogenicity of this mutation, we used several *in silico* splice site prediction programs, such as Alternative Splice Site Predictor (http://wangcomputing.com/assp/), NetGene2 (http://www.cbs.dtu.dk/services/NetGene2/), NNSPLICE 0.9 (http://www.fruitfly.org/seq_tools/splice.html), Human Splice Finder3 (http://www.umd.be/HSF/) and MaxEnt Scan (http://genes.mit.edu/burgelab/maxent/Xmaxentscan_scoreseq.html). These analyses predicted that the change weakened the donor spliced site (Figure 2b).

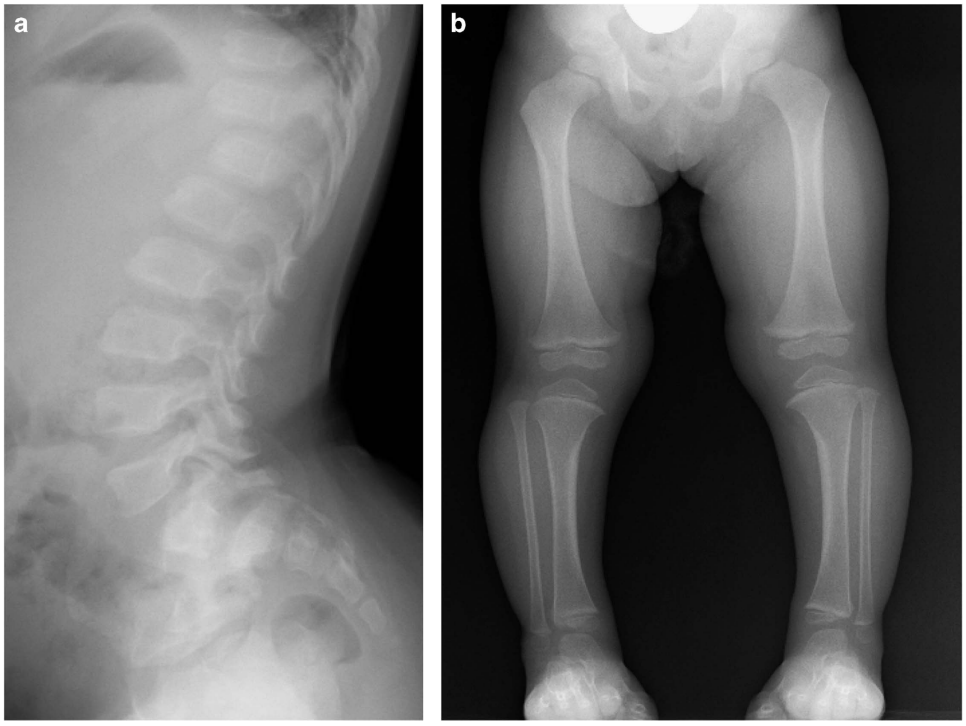

Figure 1. X-ray imaging. (**a**) A lateral spine radiograph revealed lordosis of the lumbar spine and hypoplasia of L-1. (**b**) The radiograph of the lower limbs revealed metaphyseal widening of the long bones.

Figure 2. (**a**) Electropherogram of *COL11A1* (NM_001854.3) exon 41 and flanking intron sequences showing the heterozygous germline mutation NM_001854.3:c.3168+5G > A (arrow). The DNA and corresponding amino acid sequences of wild-type and mutant *COL11A1* alleles are shown. (**b**) Predictions of the scores of splice acceptor and donor sites of *COL11A1* exon 41 of the wild-type and mutated genomic bases (arrowheads). The closed arrow indicates exon 41. The scores calculated using Alternative Splice Site Predictor, NetGene2, NNSPLICE 0.9, Human Splicing Finder3 and MaxEntScan are displayed below each splice site. A higher score predicts a strong splice site. Note that the scores of a splice donor site of exon 41 were markedly decreased by the c.3168+5G > A mutation determined using most of the prediction tools. (**c**) Left, diagrams of exon 41 and parts of flanking introns 40 and 41, the location of the c.3168+5G > A mutation (left upper) and the pET01 construct (left lower). In the pET01 construct, the intron containing the multiple cloning site (MCS) is flanked by the 5′-donor and 3′-acceptor splice sites of pre-proinsulin 5′ and 3′ exons, respectively (http://www.mobitec.com/cms/products/bio/04_vector_sys/exontrap.html). The expression of this vector sequence was driven by the promoter present in the long terminal repeat (LTR) of Rous Sarcoma Virus followed by a short stretch of a eukaryotic gene (phosphatase). The sequences containing the mutation detected in *COL11A1* intron 41 (MUT) or those that did not (WT) were cloned into the MCS of pET01. The primers used in the reverse transcription-PCR (RT-PCR) experiments within the preproinsulin 5′ and 3′ exons are indicated by the arrows (Supplementary Table S1). The length of each fragment is indicated. Right, representative results of RT-PCR analysis using HCT116 and HEK293 cells transfected with an empty pET01 vector (mock), the pET01-WT containing the WT fragment or the pET01-MUT vector containing the MUT fragment. The 301-bp transcript, including *COL11A1* exon 41 (54-bp), was detected in cells transfected with pET01-WT, whereas the 247-bp transcript without this exon was detected in mock- and pET01-MUT-transfected cells. Each transcript is indicated to the right of the gel. The asterisks indicate nonspecific bands. (**d**) Nucleotide and amino acid sequences of transcripts obtained in the minigene assay. A closed arrow denotes the sequence from *COL11A1* exon 41, and arrows denote the sequence of the preproinsulin 5′ and 3′ exons. Sequence analysis did not detect a 54-bp exonic sequence in the transcripts present in pET01-MUT-transfected cells, suggesting that the c.3168+5G > A mutation inactivated the splice donor site of *COL11A1* exon 41.

To validate these predictions, we used a functional assay that may be useful for diagnostic laboratories to quickly examine the potential pathogenic effects of sequence variants. A minigene assay was performed to determine the effect of the mutation on *COL11A1* transcript splicing.[8] A 1,678-bp genomic DNA fragment that included *COL11A1* exon 41 and its flanking sequences (parts of introns 40 and 41) was amplified by PCR with primers containing the appropriate restriction enzyme sites (Supplementary Table S1) from the patient carrying the wild-type and variant (mutated) alleles. PCR products were cloned into the Exontrap Cloning Vector pET01 (MoBiTec GmbH, Göttingen, Germany; Figure 2c); their sequences were validated using Sanger sequencing.

Because intron 41 is >10 kb, we included a part of intron 41 (1,533 bp) that may contain several cryptic splice donor sites instead of the correct donor site predicted *in silico* in the fragment used for the minigene assay. The wild-type and mutant transcripts were produced by transient transfection of empty (pET01-mock),

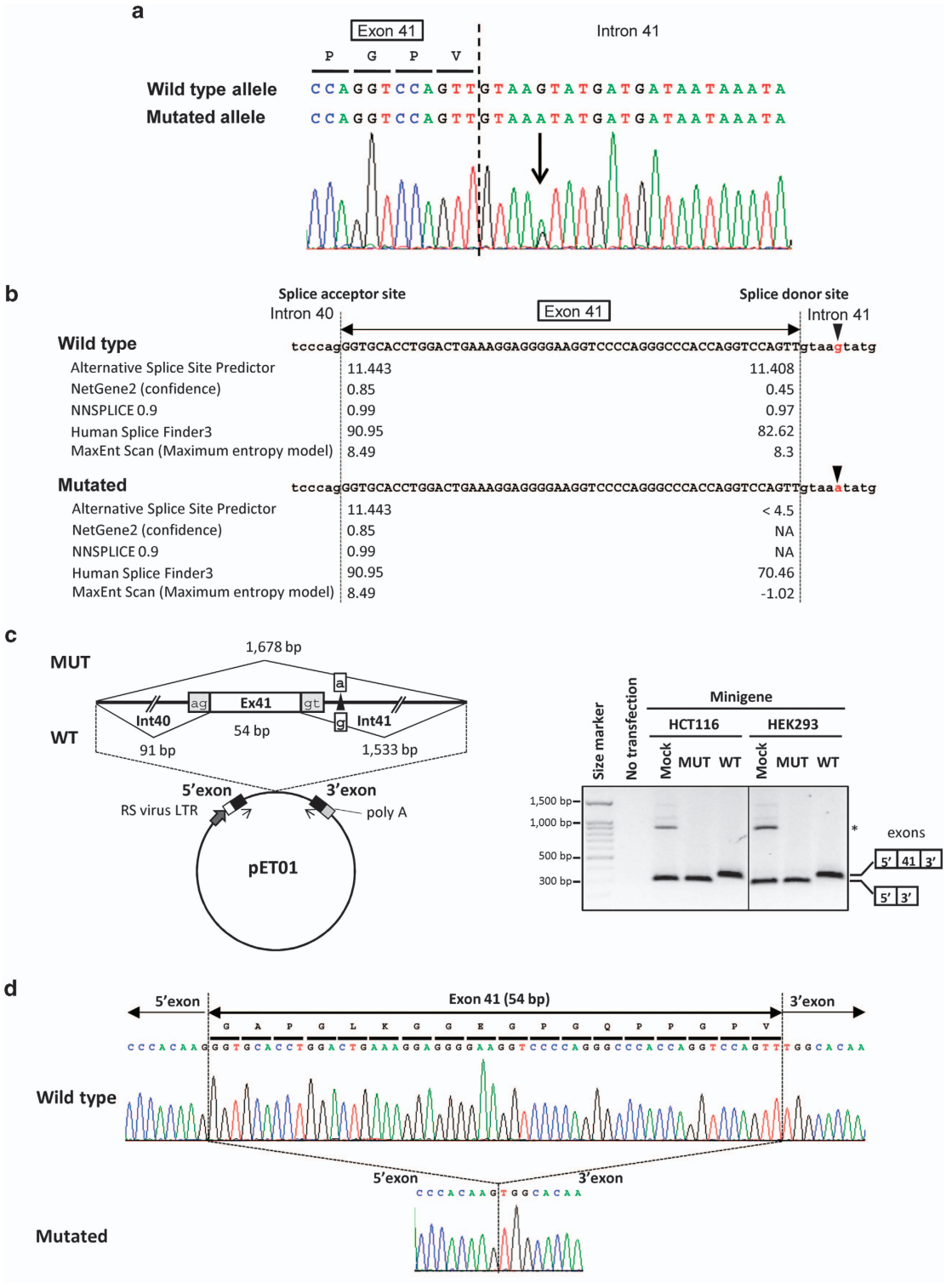

wild-type (pET01-WT) or mutant (pET01-MUT) plasmids into HCT116 or HEK293 cells using FuGENE6 (Promega, Madison, WI, USA) according to the manufacturer's instructions. Total RNA obtained from cells 48 h after transfection was subjected to reverse transcription-PCR (RT-PCR) using primers corresponding to the 5′ and 3′ exons in the pET01 vector (Supplementary Table S1). The cells that were transfected with pET01-WT produced a 301-bp band that was consistent with correct mRNA splicing (Figure 2c). In contrast, RT-PCR analysis detected a 247-bp band in cells that were transfected with pET01-MUT containing the c.3168+5G>A mutation (Figure 2c) and in cells that were transfected with the empty vector (mock). Direct sequencing of the RT-PCR products revealed that the larger fragments were observed in cells that were transfected with pET01-WT containing an insertion of 54 bp of exon 41 because of normal splicing and that cells transfected with pET01-MUT lacked this insertion (Figure 2d). These findings indicate that the c.3168+5G>A mutation disrupted the donor splice site of exon 41 and induced the skipping of the entire exon 41, encoding 18 amino acid residues. A similar result from a minigene assay has been reported from a Stickler syndrome case with a small insertion in the same intron 41 of *COL11A1* (NM_001854.3:c.3168+2_3168+3insTT).[9,10] Because only a part of intron 41 was tested in the minigene assay, we were unable to determine whether this mutation induced exon skipping, as observed in the minigene assay or activated a cryptic donor site somewhere within intron 41 to generate a larger aberrant exon. In either case, the c.3168+5G>A mutation likely affected mRNA processing and produced a misspliced transcript, although we were unable to determine whether an aberrant transcript was present in the patient's cells because COL11A1 is mainly expressed in mesenchymal cells. Cartilage and skin fibroblasts, which may express *COL11A1* mRNA, were unavailable from the affected patient.[11,12]

The use of NGS in diagnostic laboratories will facilitate the characterization of a greater number of unclassified variants detected in patients with genetic disorders. For example, a significant number of non-exonic mutations may exist within candidate genes contributing to Stickler syndrome.[11] Significant portions of the reads obtained in whole or targeted exome sequencing from outside the targeted regions[13] or complete genome capture of target genes may enhance the detection of non-exonic variants with uncertain pathogenicity. Therefore, integrated analyses using databases, bioinformatics tools, and functional studies may be critical for determining the pathogenicity of variants and facilitating differential diagnosis, appropriate therapy, and genetic counseling for patients with Stickler syndrome and related diseases.

HGV DATABASE

The relevant data from this Data Report are hosted at the Human Genome Variation Database at http://dx.doi.org/10.6084/m9.figshare.hgv.708.

ACKNOWLEDGEMENTS

We thank the patient and her family for participating in this study. This work was supported by JSPS KAKENHI Grant Numbers 26293304 (I.I.), 15K19620 (T.N.) and 26861783 (N.O.) from the Ministry of Education, Culture, Sports, Science and Technology, Japan.

COMPETING INTERESTS

The authors declare no conflict of interest.

REFERENCES

1 Stickler GB, Belau PG, Farrell FJ, Jones JD, Pugh DG, Steinberg AG *et al.* Hereditary progressive arthro-ophthalmopathy. *Mayo Clin Proc* 1965; **40**: 433–455.
2 Robin NH, Moran RT, Ala-Kokko L. Stickler syndrome In: Pagon RA, Adam MP, Ardinger HH, Wallace SE, Amemiya A, Bean LJH *et al.* (eds). *GeneReviews [Internet]*. University of Washington: Seattle, WA, USA, 2000; 1993–2015. [updated 2014 Nov 26].
3 Ahmad NN, Ala-Kokko L, Knowlton RG, Jimenez SA, Weaver EJ, Maguire JI *et al.* Stop codon in the procollagen II gene (COL2A1) in a family with the Stickler syndrome (arthro-ophthalmopathy). *Proc Natl Acad Sci USA* 1991; **88**: 6624–6627.
4 Vikkula M, Mariman ECM, Lui VCH, Zhidkova NI, Tiller GE, Goldring MB *et al.* Autosomal dominant and recessive osteochondrodysplasias associated with the COL11A2 locus. *Cell* 1995; **80**: 431–437.
5 Richards AJ, Yates JRW, Williams R, Payne SJ, Pope FM, Scott JD *et al.* A family with Stickler syndrome type 2 has a mutation in the COL11A1 gene resulting in the substitution of glycine 97 by valine in α1(XI) collagen. *Hum Mol Genet* 1996; **5**: 1339–1343.
6 Acke FR, Malfait F, Vanakker OM, Steyaert W, De Leeneer K, Mortier G *et al.* Novel pathogenic COL11A1/COL11A2 variants in Stickler syndrome detected by targeted NGS and exome sequencing. *Mol Genet Metab* 2014; **113**: 230–235.
7 Okamoto N, Naruto T, Kohmoto T, Komori T, Imoto I. A novel PTCH1 mutation in a patient with Gorlin syndrome. *Hum Genome Variation* 2014; **1**: 14022.
8 Naruto T, Okamoto N, Masuda K, Endo T, Hatsukawa Y, Kohmoto T *et al.* Deep intronic GPR143 mutation in a Japanese family with ocular albinism. *Sci Rep* 2015; **5**: 11334.
9 Richards AJ, McNinch A, Martin H, Oakhill K, Rai H, Waller S *et al.* Stickler syndrome and the vitreous phenotype: mutations in COL2A1 and COL11A1. *Hum Mutat* 2010; **31**: E1461–E1471.
10 Richards AJ, Fincham GS, McNinch A, Hill D, Poulson AV, Castle B *et al.* Alternative splicing modifies the effect of mutations in COL11A1 and results in recessive type 2 Stickler syndrome with profound hearing loss. *J Med Genet* 2013; **50**: 765–771.
11 Richards AJ, McNinch A, Whittaker J, Treacy B, Oakhill K, Poulson A *et al.* Splicing analysis of unclassified variants in COL2A1 and COL11A1 identifies deep intronic pathogenic mutations. *Eur J Hum Genet* 2012; **20**: 552–528.
12 Annunen S, Korkko J, Czarny M, Warman ML, Brunner HG, Kääriäinen H *et al.* Splicing mutations of 54-bp exons in the COL11A1 gene cause Marshall syndrome, but other mutations cause overlapping Marshall/Stickler phenotypes. *Am J Hum Genet* 1999; **65**: 974–983.
13 Samuels DC, Han L, Li J, Quanghu S, Clark TA, Shyr Y *et al.* Finding the lost treasures in exome sequencing data. *Trends Gene* 2013; **29**: 593–599.

Supplementary Information for this article can be found on the *Human Genome Variation* website (http://www.nature.com/hgv).